EXPERIMENTAL STUDY

In vivo behavior of a collagen-coated nano-hydroxyapatite enriched polycaprolactone membrane in rat mandibular defects

Sühan Gürbüz, DDS, PhD.,[1] Altan Doğan, DDS, PhD.,[1] Ayşe Karakeçili, PhD.,[2] Burcu Toközlü, DDS, PhD.[3]

[1]Department of Periodontology, Gazi University Faculty of Dentistry, Ankara-*Türkiye*
[2]Department of Chemical Engineering, Ankara University Faculty of Engineering, Ankara-*Türkiye*
[3]Department of Oral Pathology, Gazi University Faculty of Dentistry, Ankara-*Türkiye*

ABSTRACT

BACKGROUND: This research investigated the ability of fabricated collagen (COL) coated nano-hydroxyapatite (nHA) enriched polycaprolactone (PCL) membrane to facilitate new bone formation (NBF) and its biocompatibility.

METHODS: Unilateral mandibular angulus defects of 28 female 12-week-old long Evans rats were created with a trephine bur with 5 mm in diameter and divided into two groups. While the test group was treated with the membrane (M-1, M-2), the control was left as self-healing (C-1, C-2) and sacrificed at 2nd (M-1, C-1) and 8th week (M-2, C-2) postoperatively. The mandibular bone of the rats was evaluated histopathologically. Density of the regenerated bone was evaluated with PET/CT.

RESULTS: Histopathologically, NBF which started from the periphery of the defect had rich cellular character in M-1. Significantly higher NBF was found in M-2 when compared to M-1 (P=0.003). Furthermore, significantly lesser degree of inflammation was found in M-2 when compared to M-1 (P<0.05).

CONCLUSION: This study suggests that the novel COL-coated nHA-enriched PCL membrane can serve a promising design for tissue engineering as guided bone regeneration in alveolar defects.

Keywords: Biomimetic materials; collagen; guided tissue regeneration; hydroxyapatite; polycaprolactone.

INTRODUCTION

Tissue engineering and regenerative medicine (TE/RM) approach is an attractive strategy for regenerating the hierarchical structures of the periodontium, whereby periodontal tissues would be constructed in the laboratory under controlled conditions and surgically implanted.[1] Key considerations for periodontal TE/RM are the induction of cementum with perpendicularly inserting collagen (COL) fibers and bone crest on a level of 1–2 mm below the cemento-enamel junction. Preventing the gingival tissue down-growth and space for bone regeneration is called guided tissue/bone regeneration (GTR/GBR).[2,3] The use of advanced multiphasic scaffold designs that are able to guide the spatiotemporal requirements for periodontal/bone regeneration can be combined with GTR/GBR and bioactive molecules.[4,5]

Previously, poly(lactic acid),[6] poly(glycolic) acid,[7] and poly (lactic-co-gylicolic acid) (PLGA)[8] have been widely used as a carrier for periodontal TE/RM applications. Polycaprolactone (PCL) is a biodegradable polymer used, drug delivery devices have promising properties such as mechanical and biocompatible, mainly for the ability to produce porous support to be

Cite this article as: Gürbüz S, Doğan A, Karakeçili A, Toközlü B. In vivo behavior of a collagen-coated nano-hydroxyapatite enriched polycaprolactone membrane in rat mandibular defects. Ulus Travma Acil Cerrahi Derg 2023;29:1081-1090.

Address for correspondence: Sühan Gürbüz, DDS, PhD.
Gazi University Faculty of Dentistry, Ankara, Türkiye
E-mail: suhankarluk@gmail.com

Ulus Travma Acil Cerrahi Derg 2023;29(10):1081-1090 DOI: 10.14744/tjtes.2023.90673 Submitted: 14.08.2023 Revised: 25.08.2023 Accepted: 29.08.2023

used for bone repair.[9] However, it has disadvantages such as hydrophobicity, which hampers cell adhesion, which may impair the biological interactions with the medium. For these reasons, to promote the restoration of the periodontium or bone structure and its functional properties represent attracting alternative therapies.

Many bioactive materials such as hydroxyapatite (Ca10(PO4)6(OH)2), bioglass, and sintered tricalcium phosphate are widely used as bone grafts in alveolar bone regeneration. The current clinical approaches and advances in the nanotechnology and nano-biomaterials have been extensively investigated for applications in orthopedics and bone regeneration.[10] To maximize the regenerative outcome, nano-hydroxyapatite (nHAp) may be used in combination with PCL to integrate more rapidly into bone and surrounding tissues[11] and increase cell adhesion, osteogenic activity, and bone mineralization.[12] Moreover, COL-based membranes, routinely used as a barrier membrane (GTR/GBR) in the clinical practice.[4,13] Combining PCL with COL, a rapidly degrading organic protein, may be a suitable approach to reduce the enzymatic degradation of PCL and to increase biodegradability and hydrophilicity similar to extracellular matrix (ECM).[14]

Although there are various studies in the literature containing COL, nHAp, and PCL, the authors have not encountered a study that tested the biocompatibility and potential bone regeneration of a PCL-containing multifunctional membrane containing nHAp, which is coated with a COL-containing layer prepared by electrospinning method and mimics bone structure due to its porous structure. The purpose of this research was to evaluate the biocompatibility and the potential effect of fabricated COL-coated nHA enriched PCL membrane on osteogenic activity to facilitate GTR during the early stages of bone regeneration with impaired bone healing capacity in rat mandibular angulus defect.

MATERIALS AND METHODS

Materials

The PCL-based membranes used in this study have been produced by Ankara University, Faculty of Engineering, Chemical Engineering Department, Türkiye. The process of fabrication, as well as the chemical and physical characterization, has been described, previously.[12] The membranes have cylindrical shape with an 8 mm diameter and 2 mm thickness. First, the inner layer of the membrane consisted of PCL and nHAp was produced by solvent-casting/particulate leaching method.[15] NaCl particles (355–600 mm) were added to the PCL and nanoparticle hydroxyapatite solution together with solvent (dichloromethane) to create porosity in the inner layer. The solvent was evaporated and a porous structure was obtained by washing the salt with distilled water. In the second step, PCL and COL (Type I from COL calf skin) were coated on both sides of this layer by electrospinning method (Fig. 1). The solution obtained in this method was spinned on the middle layer fixed on a metal collector with a syringe and nanofibers were formed. The membranes were sterilized by γ-irradiation (25 kGy) according to Cottam's PCL sterilization[16] using Cobalt-60 under temperature 25°C (60Co) and humidity 38.7%.

Animals

An animal cohort comprised 28 female 12-week-old Long Evans rats, weighing between 200 and 250 g were used. All animals were fed with commercial rat pellets and water ad libitum and kept in separate cages under standard laboratory conditions of temperature (22±2°C) and relative humidity (50±5%) and a light/dark cycle of 12/12 h. The experimental procedures were certified by Animal Research Ethics Committee of Gazi University with an approval number of G. Ü. ET-13.05 and the ARRIVE guidelines were followed.[17] Experimental animals were purchased from GUDAM and the experiments conducted in the operating room of the GUDAM-

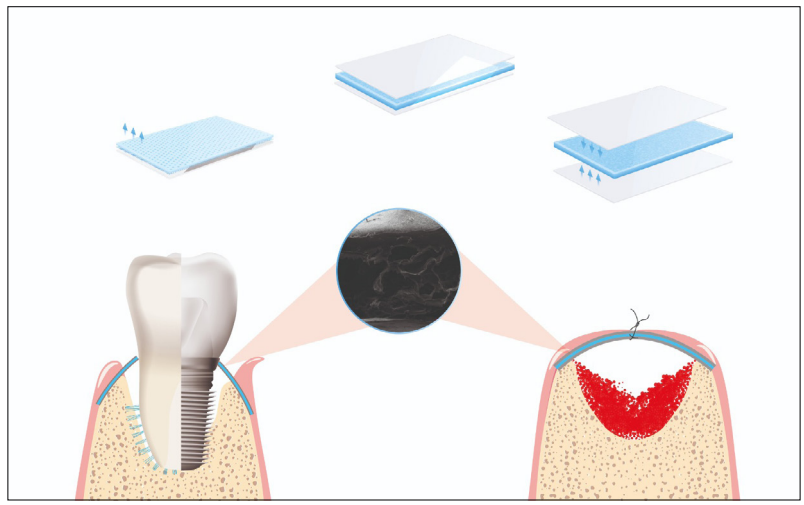

Figure 1. The graphical drawing of the membrane.

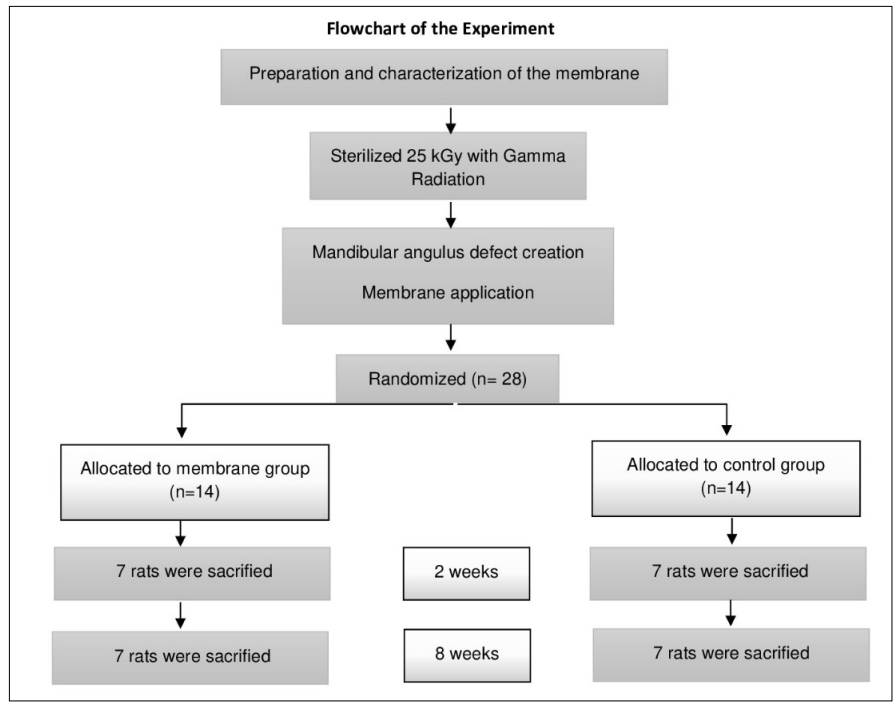

Figure 2. Flowchart of the experiment

Laboratory Animal Breeding and Experimental Research.

Experimental Design

Rats were randomly assigned to one of the following four groups. Flowchart of the experiment is shown in (Fig. 2).

1) Sham-operated (C-1) (n=7) (animals without membrane placement and sacrificed at 2 weeks)

2) Sham-operated (C-2) (n=7) (animals without membrane placement and sacrificed at 8 weeks)

3) Membrane group (M-1) (n=7) (animals with membrane placement and sacrificed at 2 weeks)

4) Membrane group (M-2) (n=7) (animals without membrane placement and sacrificed at 8 weeks)

Surgical Method

All procedures were performed under general anesthesia of 45 mg/kg ketamine HCl (Alfamine 10%, Ege Vet, Holland) and 5 mg/kg Xylazine HCl (Rompun 2%, Bayer AG, Istanbul). Each rat's weight was recorded after the skin was shaved. Rats were fed according to their weight through the oral gavage at the same time every day.

Before beginning the experimental study, the skin of the mandible was shaved and disinfected with povidine-iodine (10%). A full-thickness incision was made extending below the angle of the mandible to the alveolar bone and the periosteum was ablated. The critical size defect of 5 mm in diameter in the angulus of the mandible was made with the round stainless steel trephines. The term "critical-size defect" indicates that the lesion will not heal spontaneously during the lifetime of the rat.[18] In treated group, the membrane was placed buccal and lingual sides of the mandibulae extending 2–3 mm outside of the edge of the defect. The flap was carefully repositioned on the outer side of the membrane with absorbable 4.0 suture (Polyglactin 910, Vicryl™, Ethicon, Johnson and Johnson, USA) for the muscle and 3.0 silk suture for the skin (Ethicon, Johnson and Johnson, USA) (Fig. 3). All experiments were performed by the same operator (SG). Neither antibiotics nor anti-inflammatory drugs were administered after the surgery.

Clinical Observation

The rats were observed for signs of weight loss. Neither of the animals was lost during surgical procedure nor in the post-operative period (8 weeks). During dissection for bone harvesting, the surgical area, the soft tissue, and longitudinal section of the mandible were assessed for pus and/or abscess formation.

Histopathologic Procedures and Analysis

All samples were fixed in 10% phosphate-buffered formalin for at least 24 h. For decalcification, replacing 10% ethylenediaminetetraacetic acid solution (pH=7.4) in at 4°C every 3 days until the decalcification was achieved. After decalcification was completed, samples were washed in the tap water overnight, embedded in paraffin blocks following routine tissue processing. The tissues were sectioned on adhesive slides (Surgipath, X-tra Adhesive Microslides, Illinois, USA) in sagittal plane with a thickness of approximately 4–5 µm for hemotoxylin-eosin (H&E) staining.

The histological analysis of the inflammatory tissue response

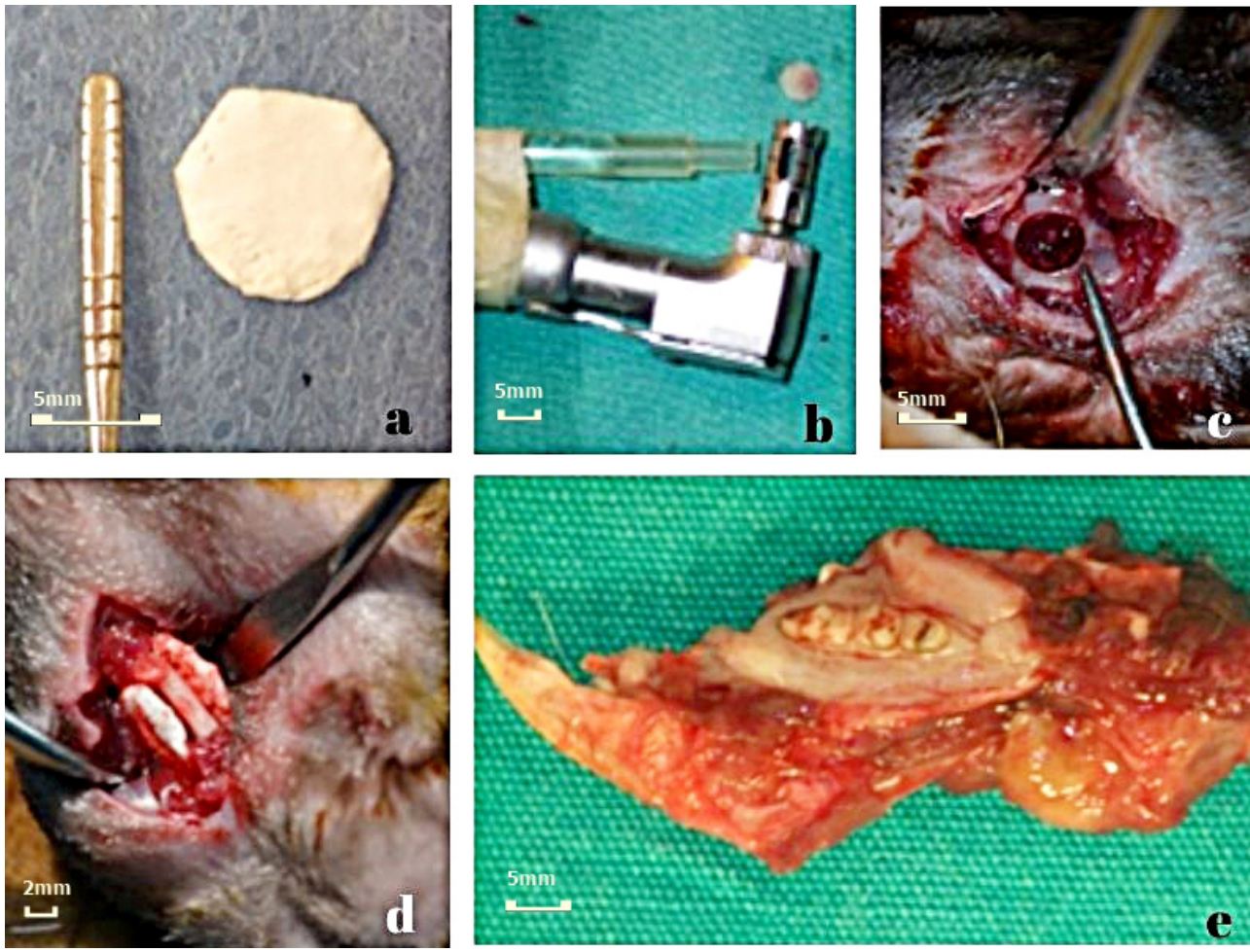

Figure 3. (a) The membrane. **(b)** Creation of the defect with a 5 mm trephine bur using saline at 125 rpm using a physiodispenser. **(c)** Defect of 5 mm diameter in left mandibular angle. **(d)** Placement of two collagen coated polycaprolactone-nHA membranes protruding 2–3 mm over the buccal and lingual surfaces of the defect. **(e)** Removal image of mandibular bone with membrane.

was performed at the Department of Oral Pathology of Gazi University, by an oral pathologist, blinded to the type of treatment with experience on animal studies and tissue reactions on a light microscopy (Leica DM 4000 B digital camera, Leica Microsystems GmbH. Wetzlar, Germany). The intensity and quality of the inflammatory response and the foreign body reaction (FBR) in the connective tissue were evaluated by the tissue inflammation score (Table 1), as described before.[19,20]

The sections per specimen representing the middle portion of the defect stained with H&E of the mandible. The amount

Table 1. New bone formation calculation and tissue response scores

New bone formation (percentage)	New bone × 100/total defect
The inflammatory density score	0: No inflammation
	1:<15 inflammatory cells per area
	2: 15–50 inflammatory cells per area
	3: 50–75 inflammatory cells per area
	4: 75 or more inflammatory cells per area
Foreign body reaction	0: Absent 1: Present
Necrosis	0: Absent 1: Present
Microorganism	0: Absent 1: Present

NBF: New bone formation; IDS: Inflammatory density score; FBR: Foreign body reaction.

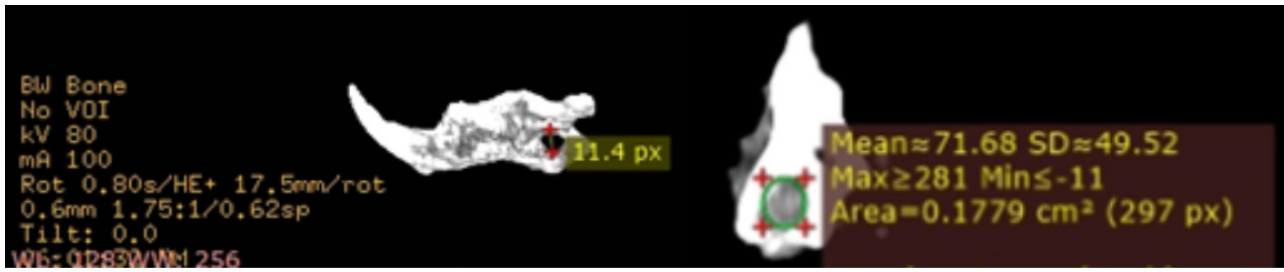

Figure 4. Calculation of HU from PET/CT images: Cross-section view of the mandibular bones.

of new bone formation (NBF) was histomorphometrically calculated as the percentage of new bone to the total defect area. Inflammatory cell infiltration in the defect area was counted in H&E sections and the inflammatory density score (IDS) was scored by a four-degree system.[19,21] FBR, necrosis, and microorganism were recorded as absent or present.

Radiographic Evaluation

Half of the rats were sacrificed at week 2 and the other half at week 8 after surgery. The mandible bone was excised and the hemi-mandibles were dissected together with the surrounding tissue and fixed in 10% buffered paraformaldehyde solution for 24–72 h. The mandibles were imaged on a 16-row multi-slice CT (Aquilion, Toshiba Medical Inc., Tustin, CA, USA) using the following parameters. To assess the regeneration intensity, the jaws were taken by fixation on a cardboard box using 0.625 mm slice thickness, 140 kilovolts, 440 milliampere, and a bone tissue filter. The samples were scanned from the base to the condyle with axial sections. The scan plane was positioned parallel to the mandibular base. The data were sent to a Centricity workstation in Digital Imaging Communication in Medicine saved on a CD-ROM-R and DICOM 3.1.4. and transferred to a standalone computer (Pentium 4, 60 GB HDD, 512Mb RAM, running Windows XP) to be readable with the viewer. DICOM images were transferred to the Radiant DICOM viewer 2020.2 and each of the computed tomography slices was analyzed quantitatively, and the density was determined as Hounsfield units (HU). All images were reconstructed in 3D and the data were evaluated with the commercially available Radiant software (Fig. 4).

Statistical Analysis

Statistical analysis was conducted using the SPSS Statistics 20 software package (IBM Corp., NY, USA). Quantitative variables are expressed as mean ± standard deviation and median (minimum–maximum) for normally and non-normally distributed variables. Data obtained from histologic analysis, intergroup comparisons of the parameters that showed normal distribution were performed using one-way analysis of variance (ANOVA), and significant differences between groups were determined using Tukey's post hoc test following Levene's test to evaluate the homogeneity of variances. The variables PET/CT results (HU) whether the parameters showed normal distribution or not were assessed using the Shapiro–Wilk test. Intergroup comparisons of parameters that did not show normal distribution were performed using the Kruskal–Wallis test, and significant differences between groups were determined using the Mann–Whitney U test. The Chi-square test was used to analyze difference between the percentage (%) for categorical variables (FBR, necrosis, and microorganism). $P < 0.05$ was accepted as statistically significant. Univariate ANOVA was used with bootstrap analysis to determine dependent quantitative variables in groups 2 and 8 weeks and for the membrane and self-healing groups according to the HU values. Multiple comparisons were evaluated with Bonferroni correction.

RESULTS

The study was completed with 28 rats. No obvious signs of systemic illness occurred during the study period.

Histopathologic Results

Microscopic images of the tissue samples examined are given in (Figures 5 and 6). After 2 weeks of healing, generation of vascular fibrous connective tissue and newly formed bone

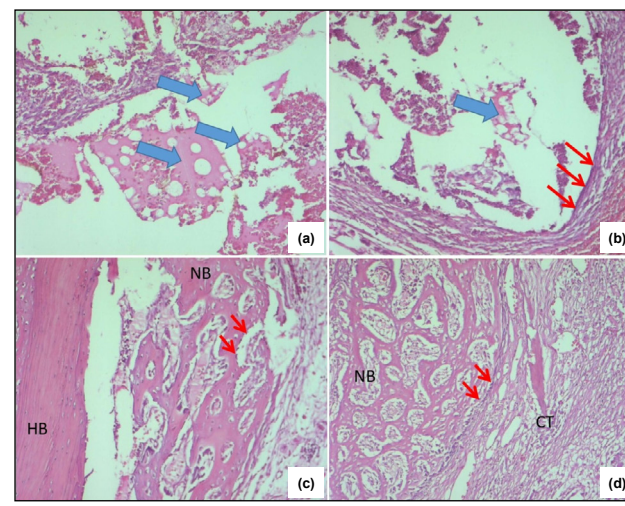

Figure 5. Histologic findings of test group at the 2nd week in test group. **(a)** Membrane (H&E stain, ×100) (blue arrow), **(b)** Membrane (blue arrows), thin fibrous capsule formation (red arrows) (H&E stain, ×100), **(c)** osteoblastic alignment (red arrows) (H&E stain, ×40), **(d)** osteoblastic alignment (red arrows) capillary rich tissue, and (k) new bone formation in rich loose, young connective tissue (H&E stain, ×40) HB: Host bone; NB: New bone formation; CT: Fibrous connective tissue.

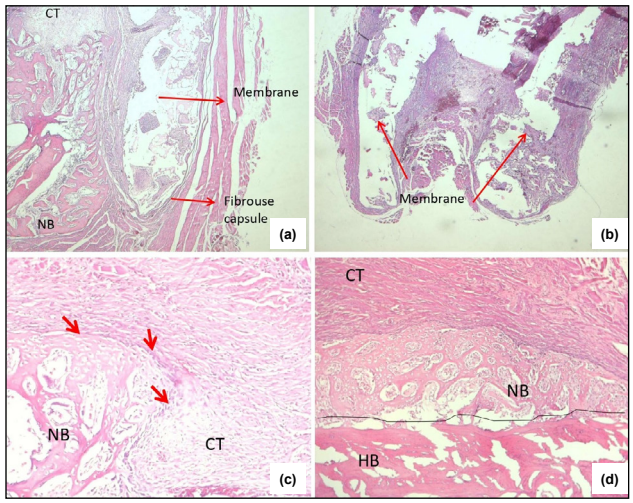

Figure 6. Histologic findings (**a**, H&E stain ×40) test group at the 2nd week (**b**, H&E stain ×20) test group at the 8 week (**c**, H&E stain ×200) control group at the 2nd week osteoblastic alignment (red arrows) (**d**, H&E stain ×100) at the 8 week. HB: Host bone; NB: New bone formation; CT: Fibrous connective tissue.

was observed through the microscope. In the M-1 group, while the NBF started from the periphery of the defect and had a cellular character (osteocyte-rich bone), NBF did not show lamellation yet, and had distinct osteoblastic rimming around it (Figures 5a-d). The defect area was isolated by the membrane and thin fibrous capsule and the membrane was not completely resorbed in all test groups (Figures 6a and b). Although almost all findings are the same as in the M-1 group, in M-2 group, the degree of inflammation has decreased and chronic inflammatory cell infiltration has become dominant. Noticed lymphoid aggregate, giant cells, and material are also monitored in M-1 group. The connective tissue has a more cellular and collagenized structure, and its bone production has increased slightly. In the C-1 group , which did not have any treatment, it was observed that the defect area was generally filled with new, vascularized, collagenized connective tissue, and that NBF was started from the periphery (Fig. 6c). Inflammatory cell infiltration and free bleeding areas were noted not very dense. No giant cell was observed. In the C-2 group, it was followed by decreased inflammation and increased bone formation compared to the previous group (Fig. 6d).

There was no statistical difference between weight and thickness of bone between groups (P<0.05). NBF was found to be 18.6% in M-1 group and 11.4% in C-1 group and no statistical difference was found between them (P>0.05). On the 8th week, NBF was found as 30% in M-2 and 16.4% in C-2 group, and the difference between them was found statistically significant (P=0.003). When the degrees of inflammation are examined in 2nd week, while 3rd degree inflammation was observed most in M-1 (57.1%), 1st degree was most in C-1 (57.1%), and the difference was found statistically significant (P=0.046). On the 8th week, there was no statistical difference between the membrane and sham-operated groups in terms of inflammation. There was no difference between the groups in terms of presence of FBR, necrosis, and microorganism, both by day and by the presence of membrane. However, necrosis was found in every group. FBR was observed in every group except the 8th week of the sham-operated group (Table 2). While microorganism was observed in both membrane and control in 2nd week, it was not observed in 8th week.

Radiographic Analyses

Radiographic evaluation with PET/CT tomography images showed radiolucencies at the defect area in all groups but indicated a significant increase in NBF in the test group at 8 weeks in comparison with at 2 weeks (P<0.05) (Fig. 7). When the mean density of the regenerated tissue was examined in the test group, the mean value was 68.9 HU at the 2nd week and 137 HU at the 8th week (P<0.05). In the control group, the mean value was 56.2 HU at the 2nd week, while the mean value was 97 HU at the 8th week, and the difference between them was statistically significant in both time point comparisons (P<0.05). According to univariate ANOVA analysis, the effects of membrane presence and time-dependent variation (2 weeks vs. 8 weeks) on HU were found to be statistically significant (P=0.001 and P<0.001, respectively). The effect of the time-dependent variation interaction with the membrane presence on HU was not found (P=0.07). About 75.7% of the change in HU was explained by the presence of membrane and temporal variation.

DISCUSSION

The theory of GTR has been described previously as an optimum technique for achieving the regeneration of periodon-

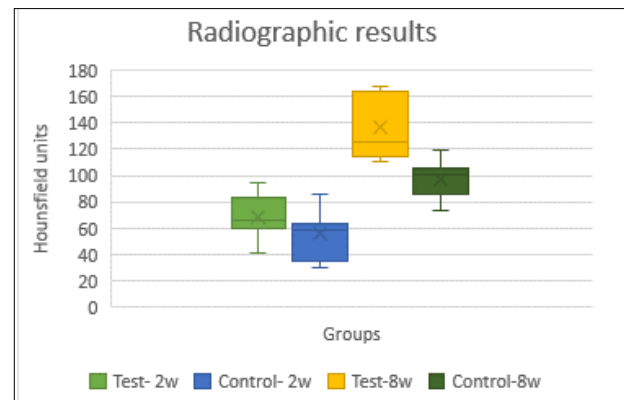

	Membrane	Self-healing	Total
2 weeks	68.9 ± 17.11a	56.21 ± 18.76a	62.55 ± 18.46
8 weeks	136.96 ± 24.05b	97.03 ± 14.78c	116.99 ± 28.24
Total	102.93 ± 40.61	76.62 ± 26.68	89.77 ± 36.28

a-c: There is no difference between membrane*day interactions with the same letter.

Figure 7. Comparison of the membrane and self-healing Hounsfield unit scores in both 2- and 8-week groups.

Table 2. Comparison of the weight of rats, the thickness of the available bone, and histopathological findings of the PCL-based membrane and control groups on weeks 2 and 8

Variables		Week 2		Week 8	
		T1 (n=7)	C1 (n=7)	T2 (n=7)	C2 (n=7)
Weight	Mean±SD	271.14±16.82	274±14	271.43±14.86	273.14±19.95
	Median (min-max)	263 (253–299)	277 (256–293)	275 (255–296)	276 (251–295)
	Significance	0.986a			
Thickness of bone	Mean±SD	0.21±0.02	0.21±0.02	0.22±0.02	0.19±0.02
	Median (min-max)	0.21 (0.18–0.23)	0.22 (0.18–0.23)	0.22 (0.2–0.25)	0.18 (0.18–0.23)
	Significance	0.145a			
New bone formation	Mean±SD	18.57±9.45	11.43±9.45	30±7.07	16.43±4.76
(Percentage)	Median (min-max)	20 (0–30)	15 (0–20)	25 (25–40)	15 (10–25)
	Significance	0.160b		0.003b	
Inflammation	Scores				
(IDS) (%)	1	0 (0.0)	4 (57.1)	0 (0.0)	2 (28.6)
	2	2 (28.6)	2 (28.6)	3 (42.9)	2 (28.6)
	3	4 (57.1)	0 (0.0)	4 (57.1)	3 (42.9)
	4	1 (14.3)	1 (14.3)	0 (0.0)	0 (00.0)
	Significance	0.046c		0.310c	
Foreign Body Reaction (%)	Absent	3 (42.9)	6 (85.7)	4 (57.1)	7 (100)
	Presence	4 (57.1)	1 (14.3)	3 (42.9)	0 (0)
Necrosis (%)	Absent	6 (85.7)	6 (85.7)	5 (71.4)	6 (85.7)
	Presence	1 (14.3)	1 (14.3)	2 (28.6)	1 (14.3)
Microorganism (%)	Absent	6 (85.7)	6 (85.7)	7 (100)	7 (100)
	Presence	1 (14.3)	1 (14.3)	0 (0)	0 (0)

IDS: Inflammation density score, One-way ANOVA test was used to compare the data with normal distribution according to the weeks of the control group and test group. Mann–Whitney U test was used for data not normally distributed. a. One-way ANOVA, Tukey test b. Mann Whitney U test c. Chi-square. PCL: Polycaprolactone.

tal/periimplant defects to prevent epithelial/connective tissue downgrowth and to provide time for the reconstruction of the periodontal tissues.[22] Similarly, GBR is a method which is utilized to increase bone ingrowth while avoiding fibrous tissue ingrowth into the grafted site.[23] Rehabilitation of periodontal and periimplant defects through barrier membranes in GTR/GBR is found to be insufficient due to the challenges of space making, clinical manageability, and cell occlusivity in clinical applications.[4,11,13] Several materials and techniques for scaffolds, one of the components of the TE principles, have been extensively investigated with different animal models for many years.[4,13,18,24,25] In our research, a membrane was designed to organize the transition of cells to the region temporospatially by combining scaffold techniques with GTR principles and adding materials that will induce bone formation into these scaffolds. The design and fabrication of multiphasic scaffolds as a promising strategy in the field of periodontal TE in the past 10 years aimed at restoring biomimetic functions to tissue-engineered hard and soft tissues.[26] Vaquette et al. (2012) reported a biphasic TE structure for periodontal regeneration with a porous PDL compartment and a hard bone compartment.[27] The interface was observed with excellent tissue integration between the bone and PDL compartments and the formation of Sharpey's fibers. Based on this study, nHAp particles in the core layer by creating a porous size that will allow the migration of bone cells into the defect. To prevent the migration of epithelial/connective tissue cells to the core layer of the defect, COL was added to increase the biocompatibility of PCL, which consists of nanofibers. In vitro study of this membrane was performed to investigate the proliferation, morphology, and differentiation of pre-osteoblastic cells (MC3T3-E1 cells) on the membrane. 3-(4,5-dimetiltiyazol-2-il)-2-5-difeniltetrazolyum bromür test (MTT) results show that the cells displayed favorable interactions with the membrane, in terms of cell proliferation and ECM production.[12] In line with this field, the aim of this study is to evaluate the potential of the bone fill and the biocompatibility of the COL coated PCL-nHAp membrane in an animal defect model. To the best of our knowledge, this is the first study to evaluate the effect of the membrane produced with

these properties on a rat mandibular angulus defect model.

Three dimensionally produced scaffolds are examined for comparison in calvaria, mandibular angle, tibia, maxillary sinus, and radius bone defects.[28] Both monocortical and bicortical (through-through) defects differ completely in the presence of osteoprogenitor cells, blood supply, and regeneration potential.[6,13,25,29-31] A critical size bone defect model effectively demonstrates the difference of bone formations.[28] Although there is no consensus about ideal critical size bone defect, rat angulus defect model was used as an experimental animal model in this study, due to low cost, small size, and well-knownness in bone TE studies.[18,31-33] In our study, the 5 mm diameter critical size defect model was carried out based on the study of Dahlin et al.[18] The advantages of this model are that the rat mandibular angulus is similar to the alveolar bone, these bicortical bone defects are not a load-bearing region, and there are no any major nerves or blood vessels around this region.[18,33] One of the difficulties we experienced during our research was that the rats had to be individually caged and fed with soft food due to the possibility of injure each other's wounds.

In the studies used this model, osteoblastic differentiation and COL production were observed at 2nd week, while severe alterations were observed between at 4 and 12 weeks.[13,25] Since the critical size defect was usually healed entirely by week 12,[10] in the present study 8th week was selected as the sacrification day to demonstrate the effectiveness of the membrane. According to our histologic and radiographic results at the 8th week, it was shown that the sacrification day was the optimum day, as there was a statistical difference between the test and control groups without complete bone fill in both groups.

Isolating the bone defect area with a barrier membrane from non-osteogenic soft tissue and creating an area that prevents membrane collapse is a crucial approach in this research area. Because of its processability and durability, including ease of thermal extrusion, PCL can be used for applications where tissue regeneration is expected to take longer and membrane collapse into the defect.[24] To improve hydrophilicity and bioactivity for GBR, composites of nHAp and PCL were combined to show enhanced ability to support cell attachment and viability.[34-36] HA releases Ca2 and PO4, which enable osteogenic cells to differentiate toward osteoblasts and increase bone regeneration. On the other hand, nHAp ceramics in clinical applications are limited due to low mechanical strength, brittleness, and fatigue failure.[37] To overcome the aforementioned concerns, nHAp/PCL-based nanocomposites would be an encouraging approach.

Several previous reports indicate the desirable bone formation with COL-coated nHAp enriched PCL membrane, newly formed bone tissue.[14,38] The histologic analysis of the present study corroborated Prosecká et al,[14] who demonstrated that nanofibers optimized the viscoelastic properties of the COL/HAp/PCL scaffold may treat bone defects with bone fill, showing that COL coated nHAp enriched PCL membrane treated samples were exhibited almost healing with new bone, allowing intense COL formation and neovascularization in interconnected pore systems. Hence, the authors suggested that the NBF in the membrane group was due to the biocompatible of the biomaterial and to a proper surface characteristics of the membranes. Moreover, Phipps et al.[39] claimed that the small pore sizes in electrospun scaffolds hinder cell infiltration in vitro and tissue-ingrowth into the scaffold in vivo. Similarly, to monitor the formation of bone tissue, PET/CT images were performed on the specimens after two different periods of implantation. Consistently with our histologic results, membranes displayed better bone fill from the edges toward the center of the defect in radiographic analysis. The bone densities according to HU of the defects were significantly higher than that of the control (sham-operated) group. Consistently with our study, Xia et al.[38] also demonstrated that the ability of the material to facilitate sustained release of BMP-2 was significantly improved after addition of HAp.

Ideal membranes should encourage NBF by resorption of the membrane with minimum acidic environment. PCL does not yield a local acidic environment during the degradation procedure compared with PLA and PLGA.[11] In the present study, it was observed that inflammation was observed mild and did not differ from the 2nd week to the 8th week in the membrane group; hence, the fabricated membranes combined with COL as a natural polymer elicited very little tissue reaction. This finding is in agreement with the results of other in vitro and in vivo studies in which blending the natural polymers with synthetic polymers.[4,11,39] Moreover, the prolonged duration of inflammation can be explained by the enzymatic activity of the host's macrophages and polymorphonuclear leukocytes due to the slow degradation of the PCL-based membrane, which was consistent with the study claimed that the degradation of PCL membranes took 3–6 months.[40] In our study, FBR was also observed in the 2nd and 8th weeks and in some membranes bacteria associated with infection in new bone have demonstrated. This result can be attributed to the fact that the membranes were partially opened from the wound edges or micromotion, or rats were not used antibiotics. At the planning of the study, it was not necessary to use antibiotics, due to the sterilized membranes and in order not to disturb the intestinal flora of the rats. As mentioned in Shim et al.'s study,[41] if the surrounding tissues are not adhered to the PCL membrane at the time of insertion, the body may show a FBR. For this reason, it is crucial that the relationship of the membrane with the surrounding tissue should be shape-fitting to minimize micromotion.

One of the disadvantages of this study was the inability to perform a more detailed radiographic examination such as micro-CT and not to be compared with various membranes in a long-term follow-up study of large animal defects. Within these limits of the study, the results have shown that the fab-

ricated COL coated nHA enriched PCL membrane exhibited a bone tissue regeneration 8 weeks following implantation with limited FBRs. To reveal the clinical potential of this membrane, which was prepared with TE/RM principles, studies are needed to compare the long-term effects of various biomaterials (eg COL, PLGA) with clinically proven effects in large animal models based on the effects obtained in this study.

CONCLUSION

The fabricated COL-coated nHA enriched PCL membrane may exhibit bone filling with limited FBR. The rat mandibular bicortical angulus defect model can be used in TE/RM field for GTR applications because of mimicking the human alveolar bone defect. The shape-fitting membranes to minimize micromotion should take into account for fabrication of the membranes.

Acknowledgments

The authors would like to thank Emre Yüksel, for his significant work and assistance in the preparation of membranes and Serkan İnal (STG Engineering, Türkiye), for his detailed graphical drawings of this study.

Ethics Committee Approval: This study was approved by the Gazi University Faculty of Dentistry Ethics Committee (Date: 03.07.2013, Decision No: G.Ü.ET-13.050).

Peer-review: Externally peer-reviewed.

Authorship Contributions: Concept: S.G., A.D., A.K.; Design: S.G., A.D., A.K.; Supervision: S.G., A.D.; Resource: S.G., A.K., B.T.; Materials: S.G., A.K., B.T.; Data collection and/or processing: S.G., B.T.; Analysis and/or interpretation: S.G., B.T.; Literature search: S.G.; Writing: S.G.; Critical review: S.G., A.D.

Conflict of Interest: None declared.

Financial Disclosure: The author declared that this study has received no financial support.

REFERENCES

1. Bartold PM, Mcculloch CA, Narayanan AS, Pitaru S. Tissue engineering: A new paradigm for periodontal regeneration based on molecular and cell biology. Periodontol 2000 2000;24:253–69. [CrossRef]
2. Nyman S, Gottlow J, Karring T, Lindhe J. The regenerative potential of the periodontal ligament: An experimental study in the monkey. J Clin Periodontol 1982;9:257–65. [CrossRef]
3. Doğan A, Özdemir A, Kubar A, Oygür T. Healing of artificial fenestration defects by seeding of fibroblast-like cells derived from regenerated periodontal ligament in a dog: A preliminary study. Tissue Eng 2003;9:1189–96. [CrossRef]
4. Bottino MC, Thomas V, Schmidt G, Vohra YK, Chu TM, Kowolik MJ, et al. Recent advances in the development of GTR/GBR membranes for periodontal regeneration--a materials perspective. Dent Mater 2012;28:703–21. [CrossRef]
5. Münchow EA, Pankajakshan D, Albuquerque MT, Kamocki K, Piva E, Gregory RL, et al. Synthesis and characterization of CaO-loaded electrospun matrices for bone tissue engineering. Clin Oral Investig 2016;20:1921–33. [CrossRef]
6. Chang PC, Liu BY, Liu CM, Chou HH, Ho MH, Liu HC, et al. Bone tissue engineering with novel rhBMP2-PLLA composite scaffolds. J Biomed Mater Res A 2007;81:771–80. [CrossRef]
7. Wikesjö UM, Lim WH, Thomson RC, Cook AD, Wozney JM, Hardwick WR. Periodontal repair in dogs: Evaluation of a bioabsorbable space-providing macro-porous membrane with recombinant human bone morphogenetic Protein-2. J Periodontol 2003;74:635–47. [CrossRef]
8. Jones AA, Buser D, Schenk R, Wozney J, Cochran DL. The effect of rhBMP-2 around endosseous implants with and without membranes in the canine model. J Periodontol 2006;77:1184–93. [CrossRef]
9. Elhassan AT, Alfakry H, Peeran SW. Reasons to seek periodontal treatment in a libyan community. Dent Med Res 2017;5:38–42. [CrossRef]
10. Chen X, Fan H, Deng X, Wu L, Yi T, Gu L, et al. Scaffold structural microenvironmental cues to guide tissue regeneration in bone tissue applications. Nanomaterials (Basel) 2018;8:960. [CrossRef]
11. Wang J, Wang L, Zhou Z, Lai H, Xu P, Liao L, et al. Biodegradable polymer membranes applied in guided bone/tissue regeneration: A review. Polymers (Basel) 2016;8:115. [CrossRef]
12. Gürbüz S, Demirtaş TT, Yüksel E, Karakeçili A, Doğan A, Gümüşderelioğlu M. Multi-layered functional membranes for periodontal regeneration: Preparation and characterization. Mater Lett 2016;178:256–9. [CrossRef]
13. Gielkens PF, Schortinghuis J, De Jong JR, Raghoebar GM, Stegenga B, Bos RR. Vivosorb®, Bio-Gide®, and Gore-Tex® as barrier membranes in rat mandibular defects: An evaluation by microradiography and micro-CT. Clin Oral Implants Res 2008;19:516–21. [CrossRef]
14. Prosecká E, Rampichová M, Litvinec A, Tonar Z, Králíčková M, Vojtová L, et al. Collagen/hydroxyapatite scaffold enriched with polycaprolactone nanofibers, thrombocyte-rich solution and mesenchymal stem cells promotes regeneration in large bone defect in vivo. J Biomed Mater Res A 2015;103:671–82. [CrossRef]
15. Thadavirul N, Pavasant P, Supaphol P. Development of polycaprolactone porous scaffolds by combining solvent casting, particulate leaching, and polymer leaching techniques for bone tissue engineering. J Biomed Mater Res A 2014;102:3379–92. [CrossRef]
16. Cottam E, Hukins DW, Lee K, Hewitt C, Jenkins MJ. Effect of sterilisation by gamma irradiation on the ability of polycaprolactone (PCL) to act as a scaffold material. Med Eng Phys 2009;31:221–6. [CrossRef]
17. Percie du Sert N, Hurst V, Ahluwalia A, Alam S, Avey MT, Baker M, et al. The ARRIVE guidelines 2.0: Updated guidelines for reporting animal research. J Cereb Blood Flow Metab 2020;40:1769–77. [CrossRef]
18. Dahlin C, Linde A, Gottlow J, Nyman S. Healing of bone defects by guided tissue regeneration. Plast Reconstr Surg 1988;81:672–6. [CrossRef]
19. Ribeiro WG, Nascimento AC, Ferreira LB, Marchi DD, Rego GM, Maeda CT, et al. Analysis of tissue inflammatory response, fibroplasia, and foreign body reaction between the polyglactin suture of abdominal aponeurosis in rats and the intraperitoneal implant of polypropylene, polypropylene/polyglecaprone and polyester/porcine collagen meshes. Acta Cir Bras 2021;36:e360706. [CrossRef]
20. Özdemir B, Kurtiş B, Tüter G, Sengüven B, Tokman B, Pınar-Özdemir S, et al. Double-application of platelet-rich plasma on bone healing in rabbits. Med Oral Patol Oral Cir Bucal 2012;17:e171–7. [CrossRef]
21. Hirshberg A, Lib M, Kozlovsky A, Kaplan I. The influence of inflammation on the polarization colors of collagen fibers in the wall of odontogenic keratocyst. Oral Oncol 2007;43:278–82. [CrossRef]
22. Karring T, Nyman S, Gottlow J, Laurell L. Development of the biological concept of guided tissue regeneration -- animal and human studies. Periodontol 2000 1993;1:26–35. [CrossRef]
23. Llambés F, Silvestre FJ, Caffesse R. Vertical guided bone regeneration with bioabsorbable barriers. J Periodontol 2007;78:2036–42. [CrossRef]
24. Dwivedi R, Kumar S, Pandey R, Mahajan A, Nandana D, Katti DS, et al. Polycaprolactone as biomaterial for bone scaffolds: Review of literature. J Oral Biol Craniofac Res 2020;10:381–8. [CrossRef]
25. Hoogeveen EJ, Gielkens PF, Schortinghuis J, Ruben JL, Huysmans MC,

Stegenga B. Vivosorb® as a barrier membrane in rat mandibular defects. An evaluation with transversal microradiography. Int J Oral Maxillofac Surg 2009;38:870–5. [CrossRef]
26. Galli M, Yao Y, Giannobile WV, Wang HL. Current and future trends in periodontal tissue engineering and bone regeneration. Plast Aesthet Res 2021;8:3. [CrossRef]
27. Vaquette C, Fan W, Xiao Y, Hamlet S, Hutmacher DW, Ivanovski S. A biphasic scaffold design combined with cell sheet technology for simultaneous regeneration of alveolar bone/periodontal ligament complex. Biomaterials 2012;33:5560–73. [CrossRef]
28. Pellegrini G, Seol Y, Gruber R, Giannobile W. Pre-clinical models for oral and periodontal reconstructive therapies. J Dent Res 2009;88:1065–76. [CrossRef]
29. Srisubut S, Teerakapong A, Vattraphodes T, Taweechaisupapong S. Effect of local delivery of alendronate on bone formation in bioactive glass grafting in rats. Oral Surg Oral Med Oral Pathol Oral Radiol Endodontol 2007;104:e11–6. [CrossRef]
30. Arslan AH, Tomruk CÖ, Meydanlı EG, Özdemir İ, Duygu Çapar G, Kütan E, et al. Histopathological evaluation of the effect of systemic thymoquinone administration on healing of bone defects in rat tibia. Biotechnol Biotechnol Equip 2017;31:175–81. [CrossRef]
31. Chang PC, Luo HT, Lin ZJ, Tai WC, Chang CH, Chang YC, et al. Regeneration of critical-sized mandibular defect using a 3D-printed hydroxyapatite-based scaffold: An exploratory study. J Periodontol 2021;92:428–35. [CrossRef]
32. Kostopoulos L, Karring T. Guided bone regeneration in mandibular defects in rats using a bioresorbable polymer. Clin Oral Implants Res 1994;5:66–74. [CrossRef]
33. Higuchi T, Kinoshita A, Takahashi K, Oda S, Ishikawa I. Bone regeneration by recombinant human bone morphogenetic protein-2 in rat mandibular defects. An experimental model of defect filling. J Periodontol 1999;70:1026–31. [CrossRef]
34. Venkatesan J, Kim SK. Nano-hydroxyapatite composite biomaterials for bone tissue engineering -- a review. J Biomed Nanotechnol 2014;10:3124–40. [CrossRef]
35. Kim HW, Knowles JC, Kim HE. Hydroxyapatite/poly (ε-caprolactone) composite coatings on hydroxyapatite porous bone scaffold for drug delivery. Biomaterials 2004;25:1279–87. [CrossRef]
36. Han J, Ma B, Liu H, Wang T, Wang F, Xie C, et al. Hydroxyapatite nanowires modified polylactic acid membrane plays barrier/osteoinduction dual roles and promotes bone regeneration in a rat mandible defect model. J Biomed Mater Res A 2018;106:3099–110. [CrossRef]
37. Abdelaziz D, Hefnawy A, Al-Wakeel E, El-Fallal A, El-Sherbiny IM. New biodegradable nanoparticles-in-nanofibers based membranes for guided periodontal tissue and bone regeneration with enhanced antibacterial activity. J Adv Res 2021;28:51–62. [CrossRef]
38. Xia Y, Zhou P, Cheng X, Xie Y, Liang C, Li C, et al. Selective laser sintering fabrication of nano-hydroxyapatite/poly-ε-caprolactone scaffolds for bone tissue engineering applications. Int J Nanomed 2013;8:4197–213.
39. Phipps MC, Clem WC, Grunda JM, Clines GA, Bellis SL. Increasing the pore sizes of bone-mimetic electrospun scaffolds comprised of polycaprolactone, collagen I and hydroxyapatite to enhance cell infiltration. Biomaterials 2012;33:524–34. [CrossRef]
40. Sun H, Mei L, Song C, Cui X, Wang P. The in vivo degradation, absorption and excretion of PCL-based implant. Biomaterials 2006;27:1735–40. [CrossRef]
41. Shim JH, Won JY, Park JH, Bae JH, Ahn G, Kim CH, et al. Effects of 3D-printed polycaprolactone/β-tricalcium phosphate membranes on guided bone regeneration. Int J Mol Sci 2017;18:899. [CrossRef]

DENEYSEL ÇALIŞMA - *ÖZ*

Kolajen kaplı nano-hidroksiapatit ile zenginleştirilmiş polikaprolakton membranın sıçan mandibular defektlerinde in vivo olarak değerlendirilmesi

Dr. Sühan Gürbüz,[1] Dr. Altan Doğan,[1] Dr. Ayşe Karakeçili,[2] Dr. Burcu Toközlü[3]

[1]Gazi Üniversitesi Diş Hekimliği Fakültesi, Periodontoloji Ana Bilim Dalı, Ankara, Türkiye
[2]Ankara Üniversitesi Mühendislik Fakültesi, Kimya Mühendisliği Bölümü, Ankara, Türkiye
[3]Gazi Üniversitesi Diş Hekimliği Fakültesi, Oral Patoloji Ana Bilim Dalı, Ankara, Türkiye

AMAÇ: Bu araştırmanın amacı yönlendirilmiş kemik rejenerasyonunu (GBR) artırmak için oluşturulmuş kolajen (COL) kaplı nano-hidroksiapatit (nHA) ile zenginleştirilmiş polikaprolakton (PCL) membranın rat mandibular defektinde yeni kemik oluşumu üzerine etkilerini ve biyouyumluluğunu değerlendirmektir.

GEREÇ VE YÖNTEM: Yirmi sekiz adet 12 haftalık dişi Long Evans sıçana tek taraflı 5 mm çaptaki trefan frez ile mandibular angulus defekti oluşturuldu ve iki gruba ayrıldı. Test grubu membran (M-1, M-2) ile tedavi edilirken, kontrol grubu ise kendiliğinden iyileşmeye (C-1, C-2) bırakıldı. Ameliyat sonrası 2. haftada (M-1, C-1) ve 8. haftada (M-2, C-2) sıçanlar sakrifiye edildi. Sıçanların mandibular kemiği histopatolojik olarak değerlendirildi. Rejenere kemiğin yoğunluğu PET/CT ile değerlendirildi.

BULGULAR: Histopatolojik olarak defektin periferinden başlayan yeni kemik oluşumu (NBF) M-1'de zengin hücresel karaktere sahipti. M-2, M-1'den anlamlı olarak daha yüksek yeni kemik oluşumuna sahipti (p=0.003). Ayrıca M-2'de, M-1'ye göre anlamlı derecede daha az inflamasyon bulundu (p<0.05).

SONUÇ: Bu çalışma, yönlendirilmiş doku rejenerasyonu prensipleri ile oluşturulan yeni üretilmiş kolajen kaplı nHA ile zenginleştirilmiş polikaprolakton membranın alveolar defektlerde doku mühendisliği için umut verici bir tasarım olabileceğini göstermektedir.

Anahtar sözcükler: Biyomimetik materyaller; doku mühendisliği; hidroksiapatit; kolajen; polikaprolakton; yönlendirilmiş doku rejenerasyonu.

Ulus Travma Acil Cerrahi Derg 2023;29(10):1081-1090 DOI: 10.14744/tjtes.2023.90673